

Microstructural characteristics of NiAl/TiC composites with high TiC content prepared by pressureless melt infiltration

M. X. GAO, Y. PAN

Department of Materials Science and Engineering, Zhejiang University, HangZhou 310027, People's Republic of China

F. J. OLIVERIA, J. L. BAPTISTA, J. M. VIEIRA

Department of Ceramics and Glass Engineering/CICECO, University of Aveiro, Aveiro 3810-193, Portugal

The ordered intermetallic compound B2-NiAl is an attractive structural material for high-temperature application due to its high melting point (1638 °C), low density (5.90 g/cm³), high Young's modulus (190 GPa), and excellent oxidation resistance at high temperature. Additionally, the thermal conductivity of NiAl is 4–8 times greater than that of Ni-based superalloys [1]. However, it is inherently brittle and has inadequate elevated temperature strength. Researchers have made efforts to incorporate a reinforcing phase in the NiAl matrix to overcome its shortcomings. Mechanical alloying, hot-pressing aided exothermic synthesis, hot-pressing and reaction synthesis, and so on for the incorporation of second phase such as TiC, Al₂O₃, TiB₂, ZrO₂, or AlN into NiAl, are the successful techniques so far [2–7]. Tuan [2] reported that the strength of NiAl/Al₂O₃ was higher than the values predicted by the rule of mixtures. Xing [7] also reported that NiAl/(0–20 vol%)TiC showed higher compressive and tensile strength from room temperature to 1000 °C than polycrystalline NiAl. However, little information is available on NiAl/ceramic with low NiAl content, which can be expected to have higher wear resistance and better high temperature properties. In the present study, pressureless melting infiltration [8, 9], a simple and economic route to produce ceramic/metal composites, is used for preparing NiAl/TiC composite with about 75 vol%TiC. The microstructural characteristics, crystalline structure properties of the composites were investigated by optical microscopes (Zeiss, Jenaphot 2000, Germany), transmission electron microscopy (TEM, Hitachi, H-9000NA, Japan), energy dispersive spectroscopy (EDS, Rontec) attached to the TEM and X-ray radiation (XRD) on Rigaku, Geigerflex/D.

In the present study, the starting materials were TiC powder (H. C. Strack, Germany, $D_{50} = 1\text{--}2 \mu\text{m}$) and stoichiometric NiAl intermetallic smelted in our laboratory. TiC powder was de-agglomerated in 2-propanol medium with WC/Co balls, then dried and sieved through a 100 mesh sieve before forming. Disk-shaped TiC powder preform of $\Phi 19 \text{ mm} \times 7 \text{ mm}$, and was uniaxially pressed in a steel die up to 32 MPa, followed by cold isostatic pressing at 200 MPa. The relative density of the as-pressed TiC was 60% of the theoretical density of TiC (4.93 g/cm³), which was determined by immersing in mercury. Infiltration experiments were performed

in a graphite furnace in argon atmosphere. A piece of NiAl was placed on the top of the as-pressed TiC preform in an alumina crucible. Taking the sintering of TiC preform before NiAl melting and infiltrating into account, the amount of the NiAl piece for the infiltration was equal to 25 vol% of the TiC preform. Infiltration schedule, heating at 25 °C/min, dwelling at 1750 °C for 5 min or for 40 min, and cooling at 10 °C/min, was used.

Experiments showed that NiAl infiltrated into the porous TiC preform completely in just 5 min at 1750 °C. The densification degree of the composite was estimated from the following equation,

$$d_{\text{TDC}} = \frac{d_{\text{RDC}}}{5.90 \times 25\% + 4.93 \times 75\%}$$

where d_{RDC} is the density of the composite measured by Archimedes method in ethyleneglycol, and 5.90 and 4.93 g/cm³ are the densities of NiAl and TiC, respectively. It has always been found that the densification degree of the composites prepared in this study was higher than 99.5%. Fig. 1 is a typical optical micrograph of NiAl/TiC composite, which is produced by the infiltration at 1750 °C × 5 min. Microstructure of NiAl/TiC produced by the infiltration at 1750 °C × 40 min was nearly identical with Fig. 1. The light grains are TiC and the gray background is NiAl. Many TiC grains are joined and TiC and NiAl are well bonded forming a co-continuous three-dimensional interpenetrating network of ceramic and intermetallic phase. No distinct voids or interstice in the interface of TiC and NiAl phases were observed under the optical microscope. Limited small pores (dark dots as in Fig. 1) are mostly in intragranular position inside TiC grains, which might have originally existed or the pull-outs caused by polishing. The infiltration ability of liquid NiAl in porous TiC preform proved adequate to form dense and defect-free composites. XRD analysis confirmed that the composite has only two phases, the original NiAl and TiC. Fig. 2a and b are the bright field TEM images of NiAl/TiC composite by infiltration at 1750 °C × 40 min obtained in NiAl crystal zone axis of $\langle 1\bar{1}\bar{3} \rangle$, which isolated dislocation heads, lines, and dipoles can clearly be seen in NiAl. The dislocation morphologies were quite similar to those in the slow cooled pure NiAl reported by Ghosh [10]. It should

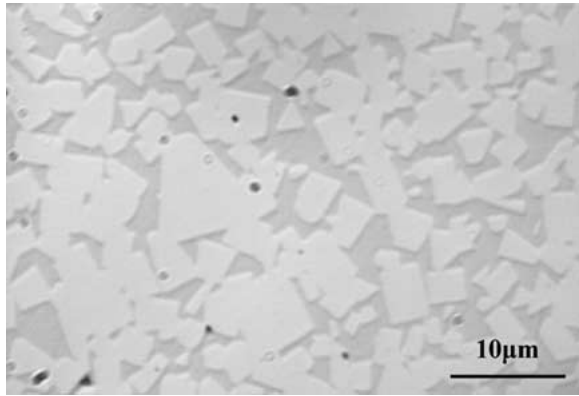


Figure 1 Typical optical micrograph of NiAl/TiC composite (by 1750 °C × 5 min infiltration).

be noted that not many dislocations were created in NiAl phase after infiltration although the thermal expansion coefficient of NiAl ($15.1 \times 10^{-6} \text{ K}^{-1}$) and TiC ($7.7 \times 10^{-6} \text{ K}^{-1}$) are quite different. The thermal stress in NiAl after cooling is not high, so few dislocations were created. This can be attributed to the high thermal conductivity ($70\text{--}80 \text{ Wm}^{-1} \text{ K}^{-1}$) of NiAl and relaxation of NiAl crystal at high temperature in the early stage of cooling. The dislocation was brought to extinction by tilting without moving the sample from $\langle 1\bar{1}\bar{3} \rangle$, as is shown in Fig. 2c (the dark dots are EDS detection positions). Another interesting discovery was that in the whole field of the TEM image containing several NiAl ligaments and TiC grains, the selected area diffraction pattern of different NiAl ligaments was almost identical. This finding infers that different NiAl ligaments in the area, with several TiC distributed grains, belong to the same crystalline grain or are oriented in

the same preferred direction. In fact, grain boundaries in the NiAl phase were not seen by optical microscopy even when the composite was carefully polished using $1 \mu\text{m}$ diamond paste and acid etched by a solution of $33\% \text{HNO}_3 + 33\% \text{CH}_3\text{CO}_2\text{H} + 1\% \text{HF} + 33\% \text{H}_2\text{O}$, a procedure which works very well for NiAl to distinguish the grain boundary in other situations without infiltration involved. The slow cooling rate of $10 \text{ }^\circ\text{C}/\text{min}$, after infiltration, in the present study allowed for the crystallization and complete grain growth of the intermetallic phase, and the crystallization front moved forward freely until hitting a TiC grain, and thus stopped by the grain, left an interface between NiAl and TiC rather than the grain boundary of NiAl.

The effect of the infiltration times on the solubility of TiC and NiAl on each other was studied by the compositional measurements in both TiC grains and NiAl phase using EDS, and the results are summarized in Table I. Each value is the average of at least 6–8 tests on several areas of the same situation. The results show that TiC partially dissolved in NiAl phase. There is just a slight decreasing trend of Ti concentration in NiAl ligaments away from the interface of NiAl and TiC to the middle of NiAl ligaments. Ti concentration in NiAl ligaments was nearly homogeneous. However, the Ti concentration in NiAl increases with increasing infiltration time. Small quantity of Al and trace Ni, which might enter into TiC by diffusion or reaction, were also detected in the outer layer of TiC grains, whereas nearly no Ni and Al were detected in the center of TiC grains. The mutual dissolution of an intermetallic and a ceramic favors the formation of a satisfactory boundary, and may be the main reason for the good wetting behavior of TiC by the NiAl melt.

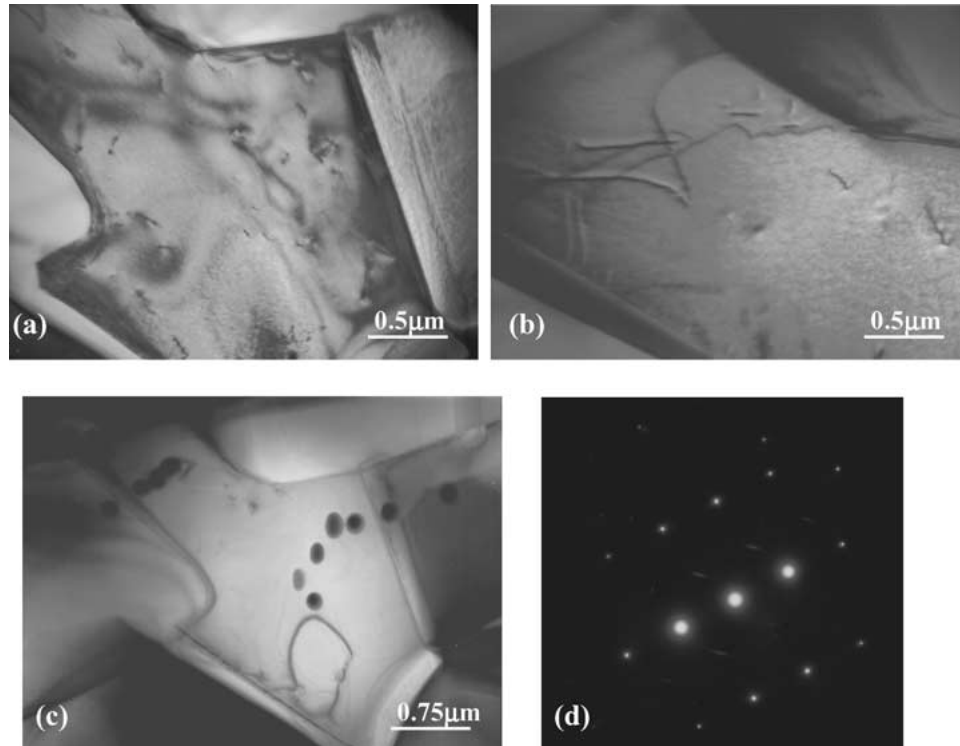


Figure 2 TEM micrographs (bright field) of NiAl/TiC composite (by 1750 °C × 40 min infiltration): (a) and (b) dislocation morphologies in NiAl phase on zone axis of $\langle 1\bar{1}\bar{3} \rangle$; (c) dislocation lines in image as (a) disappeared by deviation from $\langle 1\bar{1}\bar{3} \rangle$ zone axis (the dark dots are EDS detection positions); (d) micro-diffraction pattern of NiAl phase on zone axis of $\langle 1\bar{1}\bar{3} \rangle$.

TABLE I The nominal compositions (at.%) in NiAl phase and TiC grain of NiAl/TiC composites

Infiltration condition	Positions	Ti	Ni	Al
1750 °C × 5 min	TiC (outer layer)	98.7	0.4	0.9
	NiAl	1.2	48.5	50.3
1750 °C × 40 min	TiC (outer layer)	98.5	0.4	1.1
	NiAl	2.2	48.5	49.3

In conclusion, pressureless melt infiltration is an effective method to produce dense high TiC content NiAl/TiC composites. Beside the original NiAl and TiC phases, no new phase is formed in the infiltration process. Low density of dislocations formed NiAl phase in the composites. NiAl ligaments in an area containing several TiC grains in the composites belong to the same crystalline grain. The mutual dissolution of TiC in NiAl increased with the infiltration time. The dissolution led to the two phases being well bonded.

Acknowledgments

This work is supported by National Natural Science Foundation of China (grant no. 50272062) and by GRICES-The Institute of International Science and Technology Cooperation of Portugal and Ministry of

Science and Technology, People's Republic of China. The authors would like to thank Dr. Yang Li for her participation in the TEM investigations.

References

1. R. D. NOEBE, R. R. BOWMAN and M. V. NATHAL, *Int. Met. Rev.* **38** (1993) 193.
2. W. H. TUAN and Y. P. PAI, *J. Amer. Ceram. Soc.* **82** (1999) 1624.
3. K. KRIVOROUTCHKO, T. KULIK, H. MATYJA, V. K. PORTONY and V. I. FADEEVA, *J. Alloy and Comp.* **308** (2000) 230.
4. J. T. GUO, D. T. JIANG, Z. P. XING and G. S. LI, *Mater. Design* **18** (1997) 357.
5. S. M. BARINOV and V. YU. EVDOKIMOV, *Acta Metall. Mater.* **41** (1993) 801.
6. J. D. WHITTENBERGER, E. ARZT and M. J. LUTON, *J. Mater. Res.* **5** (1990) 2819.
7. Z. P. XING, J. T. GUO, Y. F. HAN and L. G. YU, *Metall. Mater. Trans. A* **28** (1997) 1079.
8. Y. PAN and K. W. SUN, *J. Mater. Sci. Tech.* **16** (2000) 387.
9. R. SUBRAMANIAM and J. H. SCHENEIBEL, *Mater. Sci. Eng. A* **244** (1998) 103.
10. B. GHOSH and M. A. CRIMP, *ibid. A* **239/240** (1997) 142.

Received 23 July 2003

and accepted 4 March 2004